Redox Biology 8 (2016) 59–67

Contents lists available at ScienceDirect

Redox Biology

journal homepage: www.elsevier.com/locate/redox

Research paper

Cellular and subcellular oxidative stress parameters following severe spinal cord injury

Nishant P. Visavadiya [a,1], Samir P. Patel [a,1,*], Jenna L. VanRooyen [a], Patrick G. Sullivan [b], Alexander G. Rabchevsky [a]

[a] Spinal Cord and Brain Injury Research Center, Department of Physiology, University of Kentucky, Lexington, KY 40536-0509, USA
[b] Spinal Cord and Brain Injury Research Center, Department of Anatomy & Neurobiology, University of Kentucky, Lexington, KY 40536-0509, USA

ARTICLE INFO

Article history:
Received 30 November 2015
Received in revised form
24 December 2015
Accepted 29 December 2015
Available online 30 December 2015

Keywords:
4-Hydroxynonenal
3-Nitrotyrosine
Protein carbonyl
ROS
RNS
Mitochondria

ABSTRACT

The present study undertook a comprehensive assessment of the acute biochemical oxidative stress parameters in both cellular and, notably, mitochondrial isolates following severe upper lumbar contusion spinal cord injury (SCI) in adult female Sprague Dawley rats. At 24 h post-injury, spinal cord tissue homogenate and mitochondrial fractions were isolated concurrently and assessed for glutathione (GSH) content and production of nitric oxide ($NO^{\bullet}$), in addition to the presence of oxidative stress markers 3-nitrotyrosine (3-NT), protein carbonyl (PC), 4-hydroxynonenal (4-HNE) and lipid peroxidation (LPO). Moreover, we assessed production of superoxide ($O_2^{\bullet-}$) and hydrogen peroxide (H_2O_2) in mitochondrial fractions. Quantitative biochemical analyses showed that compared to sham, SCI significantly lowered GSH content accompanied by increased $NO^{\bullet}$ production in both cellular and mitochondrial fractions. SCI also resulted in increased $O_2^{\bullet-}$ and H_2O_2 levels in mitochondrial fractions. Western blot analysis further showed that reactive oxygen/nitrogen species (ROS/RNS) mediated PC and 3-NT production were significantly higher in both fractions after SCI. Conversely, neither 4-HNE levels nor LPO formation were increased at 24 h after injury in either tissue homogenate or mitochondrial fractions. These results indicate that by 24 h post-injury ROS-induced protein oxidation is more prominent compared to lipid oxidation, indicating a critical temporal distinction in secondary pathophysiology that is critical in designing therapeutic approaches to mitigate consequences of oxidative stress.

1. Introduction

Traumatic spinal cord injury (SCI) includes primary mechanical and secondary pathophysiological mechanisms of injury which ultimately cause motor, sensory and/or autonomic dysfunction. The initial insult primarily elicits tissue pathology at the injury epicenter. A number of secondary injury events follow which cause the damage to spread, including ischemia/reperfusion injury, inflammatory processes, edema, reactive oxygen/nitrogen species (ROS/RNS) generation, glutamate-mediated excitotoxicity, intracellular calcium accumulation, activation of proteases and caspases, as well as cellular necrosis and apoptosis around the injury epicenter [1–6]. SCI triggers a rapid increase in extracellular glutamate concentrations which precipitates calcium influx into cells via voltage-gated ion channels [7]. Elevated intracellular calcium is consequently taken up into mitochondrial compartments, leading to a failure of aerobic energy metabolism, inhibition of ATP synthesis, decrease in mitochondrial membrane potential, increased generation of ROS/RNS, and onset of mitochondrial permeability transition; all of which constitute mitochondrial dysfunction [8–10].

Previous studies have documented that by 24 h following contusion SCI, oxidative stress markers specific to lipid and protein oxidation, namely 4-hydroxynonenal (4-HNE), 3-nitrotyrosine (3-NT) and protein carbonyl (PC) formation, all increase in injured tissue homogenates [11–13] and in isolated mitochondria [9,14]. However, there has never been a comparative assessment of oxidative stress parameters in cellular versus subcellular fractions following contusion SCI, concurrently. Accordingly, the present study was designed to provide a comprehensive assessment of free radical production and free radical-mediated adduct formation (i.e., PC, 3-NT and 4-HNE) in tissue homogenate and mitochondria following acute severe contusion SCI in rats. In summary, compared to lipid oxidation, acute ROS-induced protein oxidation appears to be a key target to mitigate consequences of injury-induced oxidative stress.

* Correspondence to: Spinal Cord and Brain Injury Research Center (SCoBIRC) B461, Biomedical & Biological Sciences Research Building, 741 South Limestone Street, Lexington, KY 40536-0509, United States.
E-mail address: skpate2@uky.edu (S.P. Patel).
[1] These authors contributed equally to this study.

http://dx.doi.org/10.1016/j.redox.2015.12.011
2213-2317/

2. Materials and methods

2.1. Spinal cord injury

Spinal cord injury was carried out on adult female Sprague-Dawley rats (Harlan Labs, IN) weighing 225–250 g. Animals were housed in a core facility at the University of Kentucky and allowed access to water and food *ad libitum*. All animal procedures were approved by the University of Kentucky Institutional Animal Care and Use Committee and according to NIH guidelines. Prior to injury, rats were anesthetized with Ketamine (80 mg/kg i.p., Fort Dodge Animal Health, Fort Dodge, IA) and Xylazine (10 mg/kg i.p., Lloyd Laboratories, Shenandoah, IA). A dorsal laminectomy was performed at the 12th thoracic vertebra to expose the first and second lumbar (L1/L2) spinal cord levels using published methods [15,16]. Spinal cord contusions ($n=6$) were performed using the well-characterized Infinite Horizon impactor device (PSI, Lexington, KY) at 250 kDyn force [17]. Control sham rats ($n=6$) received laminectomy only at the 12th thoracic vertebra, but no injury was performed. After injury, the wound was irrigated with saline, the muscles sutured together in layers with 3–0 Vicryl (Ethicon, Inc., Somerville, NJ), and the skin layers were closed with wound clips (Stoelting Co., Wood Dale, IL). Hydrogen peroxide and betadine were used to clean the wound area and animals injected (s.c.) with pre-warmed lactated Ringer's solution (10 ml split into 2 sites bilaterally) and Cefazolin (33.3 mg/kg) before returned to their cages with food and water *ad libitum*. Upon regaining consciousness, both sham and injured rats received Buprenorphine-HCl (0.03 mg/kg; Reckitt Benckiser Pharmaceuticals Inc. Richmond, VA) (s.c.) every 8 h.

2.2. Preparation of tissue homogenate and mitochondrial fractions

At 24 h post-injury, all sham and injured animals were deeply anesthetized with CO_2, decapitated, and a 1.5 cm segment of spinal cord at the L1/L2 spinal level centered on the injury site was rapidly dissected and placed in an ice cold dissecting plate containing isolation buffer consisting of 1 mM EGTA (215 mM mannitol, 75 mM sucrose, 0.1% BSA, 20 mM HEPES, 1 mM EGTA, and pH adjusted to 7.2 with KOH) [14,16]. The spinal cord tissue homogenate was prepared using a Potter-Elvehjem homogenizer containing 2 mL of ice-cold isolation buffer, and then 400 μl of tissue homogenate was frozen immediately in liquid nitrogen for biochemical analyses. To isolate the mitochondria, the remaining tissue homogenate was centrifuged twice at $1400 \times g$ for 3 min at 4 °C to obtain a pellet containing the nuclear fraction (NU). The supernatant (cytosolic fraction: CY) was re-centrifuged at $13{,}000 \times g$ at 4 °C for 10 min and the pellet was subsequently re-suspended and placed into a nitrogen cell disruption chamber (1200 psi, 10 min, 4 °C) to release synaptosomal mitochondria, producing the mitochondrial fraction. The mitochondrial fraction was then centrifuged at $13{,}000 \times g$ for 10 min and resultant mitochondrial pellet was washed in isolation buffer without EGTA and centrifuged for 10 min at $10{,}000 \times g$ at 4 °C. The final purified mitochondrial pellet was resuspended in 50 μl isolation buffer without EGTA. The protein concentration of total homogenate and mitochondrial fraction was measured using the BCA protein assay kit.

For oxidative stress profiles, $O_2^{\bullet -}$ and H_2O_2 production assays were carried out in the mitochondrial fraction while other assays were carried out in both tissue homogenate and mitochondrial fraction. This is due to the fact that while ROS are generated in multiple compartments, the vast majority of cellular ROS (estimated at approximately 90%) can be traced back to the mitochondria in which ROS are generated as by-products of cellular metabolism. Further, the non-mitochondrial ROS released or formed in the cytosol are buffered generally under strong reducing conditions by intracellular thiols, particularly glutathione (GSH) and thioredoxin ($TRXSH_2$) by the activities of their reductases. Hence, the mitochondrial electron transport chain contains several redox centers that leak electrons to oxygen, constituting the primary/major source of ROS in tissue [18–21].

2.3. GSH measurements

Reduced form of glutathione (GSH) content was measured using the fluorescent probe monochlorobimane (MCB) as described [22]. Tissue homogenate or mitochondria (2 μg/μl) were incubated in 100 μM MCB and 1 U/ml GST reaction mixture for 30 min at 37 °C in the dark. The reaction samples were then centrifuged at $8000 \times g$ for 8 min. Finally, the fluorescence of tagged GSH in each supernatant was measured using a fluorescence reader (excitation=380 nm; emission=470 nm). Briefly, the MCB Glutathione Detection Kit utilizes MCB dye that has a high affinity for reduced GSH. The unreacted dye is virtually non-fluorescent. After glutathione-S-transferase (GST)-catalyzed reaction of the dye with GSH, the resulting blue fluorescence intensity reflects the amount of GSH present in the samples.

2.4. Lipid peroxidation measurements

Tissue homogenate or mitochondria (100 μg/100 μl assay system) were incubated in eppendorf tubes containing 10% trichloroacetic acid (TCA). Following subsequent addition of 0.67% thiobarbituric acid (TBA), tubes were placed in a boiling water-bath for 20 min and then centrifuged at $3000 \times g$ for 10 min. The amount of malondialdehyde (MDA), present as thiobarbituric acid reactive substances (TBARS) formed in the supernatant, was measured at 532 nm using the molar extinction coefficient of $1.56 \times 10^5\ M^{-1}\ cm^{-1}$ [23].

2.5. Nitric oxide measurements

Tissue homogenate or mitochondria (100 μg/100 μl assay system) were incubated with a reaction mixture containing Griess reagent (1% sulfanilamide, 2% HCl and 0.1% naphthyl ethelene diamine dihydrochloride) and vanadium (III) chloride–based reduction. Vanadium (III) in dilute acid solution causes reduction of nitrate to nitrite. The absorbance of the chromophore formed during diazotization of the nitrite with sulfanilamide, and subsequent coupling with naphthylethelene diamine, was read at 540 nm as described [24].

2.6. Immunoblots of tissue homogenates and mitochondria

Proteins (20 μg) from the various spinal cord fractions were suspended in Laemmli buffer under reducing conditions (100 mM DTT) and then separated by SDS–PAGE using Criterion 4–20% Tris–HCl (10–250 kD) gel (Bio-Rad, Hercules, CA). Proteins captured by western blot gels were trans-blotted onto polyvinylidene difluoride (PVDF), blocked with 5% nonfat dry milk for an hour at room temperature, and then incubated at 4 °C overnight in a primary antibody solution. Alternatively, detection of PC formation was performed according to published methods [25] using an OxyBlot kit (cat #S7150; Millipore Inc). The antibodies used for western blots were 3-nitrotyrosine rabbit polyclonal (3-NT – 200 nl/ml; cat #9691; Cell Signaling technology Inc.), 4-hydroxynonenal (mouse monoclonal HNE – 150 ng/ml; cat # HNEJ-2; JaICA Co., Ltd) and rabbit polyclonal (HNE – 100 nl/ml; cat #HNE11-S; alpha-diagnostic international), β-actin mouse monoclonal (25 ng/ml, cat #A2228; Sigma-Aldrich Inc.) and voltage-dependent anion channel rabbit polyclonal (VDAC; 150 ng/ml; cat

#PA1-954A; Thermo Scientific Inc). For secondary antibodies, peroxidase-conjugated affinipure goat anti-mouse IgG and goat anti-rabbit IgG were used (cat #115-035-166 and 111-035-144, respectively; Jackson ImmunoResearch laboratories, Inc). For re-probing western blots, PVDF membranes were stripped (Restore PLUS Stripping Buffer, Cat #PI-46430; Thermo Scientific) prior to blocking and incubation with a different primary antibody.

2.7. Superoxide ($O_2^{\bullet -}$) measurements in mitochondria

Formation of $O_2^{\bullet -}$was measured using 2-,7-dichlorodihydro-fluorescin diacetate ($DCFH_2$-DA) fluorescent probe, as described previously [25]. Mitochondria were incubated in KCl-based respiration buffer (125 mM KCl, 2 mM $MgCl_2$, 2.5 mM KH_2PO_4, 20 mM HEPES and 0.1% bovine serum albumin, pH 7.2) containing oxidative substrates pyruvate (5 mM) and malate (2.5 mM) (P/M) with 10 μM $DCFH_2$-DA and 5 U/ml horseradish peroxidase (HRP). Thereafter, the changes in DCF fluorescence were monitored after 10 min at 37 °C at 485-nm excitation and 520-nm emission filters using a Biotek Synergy HT plate reader (Winooski, VT).

2.8. Hydrogen peroxide (H_2O_2) measurements in mitochondria

Production of H_2O_2 in mitochondria was measured using the Amplex Red fluorescent probe, as described previously [18,26]. Isolated mitochondria were incubated in KCl-based standard respiration buffer containing 5 mM pyruvate + 2.5 mM malate (P/M) as oxidative substrates with subsequent addition of 1 μM Amplex red and 0.25 U/ml HRP at 30 °C. Fluorescence of the oxidized probe was measured in a spectrofluorometer (excitation = 530 nm; emission = 590). Standard curves were obtained by adding known amounts of H_2O_2 to standard assay medium in the presence of the reactants (Amplex red/HRP), which were linear up to 4 μM.

2.9. Statistical analysis

Data from biochemical and western blot assessments were analyzed by unpaired Student's *t*-tests using GraphPad Prism 6 (GraphPad Software, Inc). Differences were considered significant if $p \leq 0.05$.

3. Results

Consistent with our previous studies [15,16], injury parameters did not vary among animals [Force (kDyn) = 260.33 ± 1.99; displacement (μm) = 1510.50 ± 64.89; velocity (mm/sec) = 122.00 ± 1.89]. At 24 h following SCI or sham operation, anti-oxidant parameters were assessed with respect to GSH content and oxidative stress parameters in terms of production of free radicals ($O_2^{\bullet -}$, $NO^{\bullet}$ and H_2O_2), as well as markers of oxidative damage (PC, 3-NT,4-HNE and LPO).

3.1. SCI alters anti-oxidant and oxidative stress parameters at cellular and subcellular levels

3.1.1. Effects of SCI on GSH content

At 24 h after SCI there was a significant depletion ($p < 0.05$ and $p < 0.01$) of GSH content in tissue homogenate (~19%) and mitochondrial (~24%) fractions, respectively (Fig. 1). It should be noted that the GSH content in sham mitochondria was ~40% lower than in sham tissue homogenate, indicating relatively weaker reducing conditions in mitochondria that neutralize free radicals compared to that in tissue homogenates.

3.1.2. Effects of SCI on $NO^{\bullet}$ production

Total $NO^{\bullet}$ levels in spinal cord fractions were measured as an indicator of oxidative stress and/or inflammatory responses. Mitochondrial fraction from sham groups showed higher (~60%) $NO^{\bullet}$ levels compared to tissue homogenate indicating potentially increased RNS-induced oxidative stress in mitochondria even in normal conditions. Notably, at 24 h post-SCI, total $NO^{\bullet}$ levels in both tissue homogenate (~66%) and mitochondrial (~58%) fractions were significantly ($p < 0.01$) higher compared to shams (Fig. 2).

3.1.3. Effects of SCI on oxidative stress markers

Quantification of oxidative stress markers in tissue homogenate and mitochondrial fractions were assessed by western blot analyses. Qualitative differences in levels of 3-NT are shown in Fig. 3A and B; importantly, 3-NT formation was observed prominently in the SCI group as a single band at ~95 kDa protein level in both the fractions (indicated by arrows). Quantification of 3-NT levels using β-actin as a loading control showed significantly increased 3-NT levels after SCI in both the fractions compared shams (Fig. 3C and D). Interestingly, however, the increase in 3-NT levels following SCI was more pronounced in the mitochondrial fraction (~73%) than tissue homogenate (~23%), indicating relatively higher protein nitrosylation in mitochondria following SCI, possibly due to higher $NO^{\bullet}$ levels in mitochondria in shams as well as SCI groups. On the

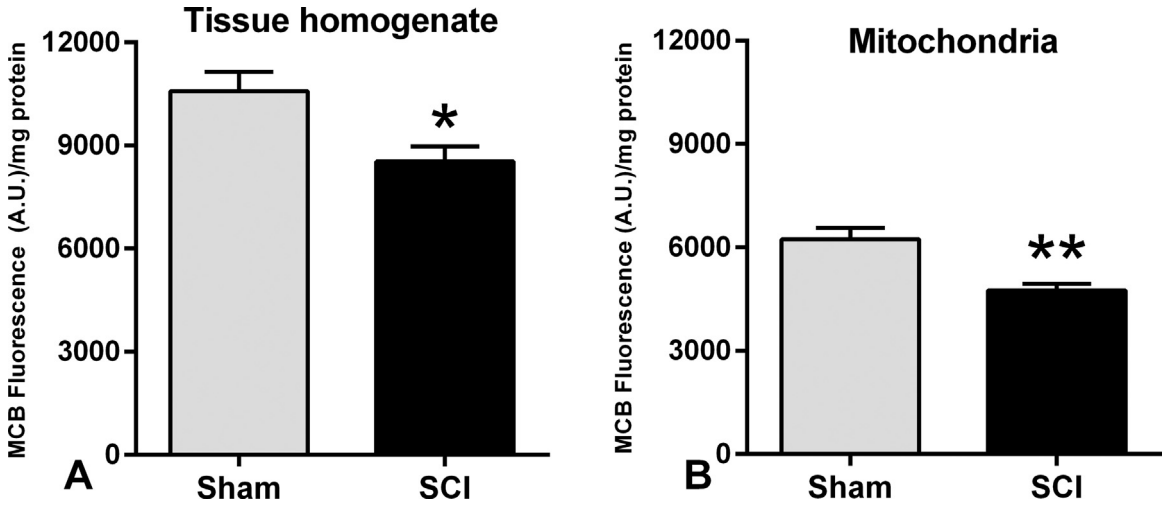

Fig. 1. GSH content was measured using the fluorescent probe MCB with GST reaction and was found to be significantly decreased 24 h after SCI in spinal cord tissue homogenate (A) and mitochondria (B) compared to Shams. Bars represent group means ± SEM, $n = 6$/group. $^{*}p < 0.05$ and $^{**}p < 0.01$.

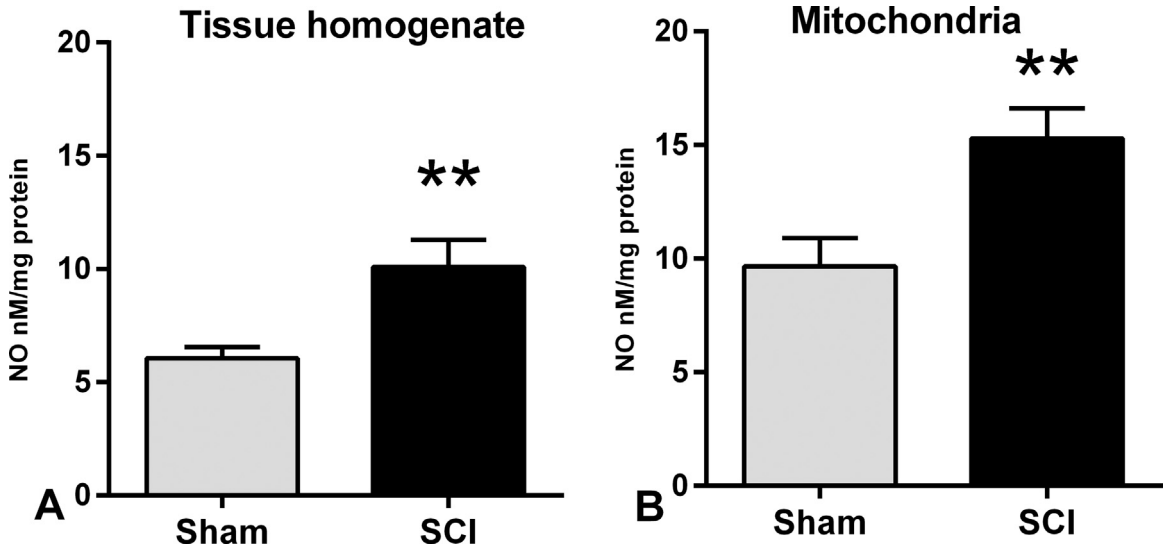

Fig. 2. $NO^{\bullet}$ levels were assessed by standard Griess reagent and vanadium (III) chloride–based reduction assay. Spinal cord tissue homogenate (A) and mitochondria (B) showed significantly increased $NO^{\bullet}$ levels 24 h following SCI compared to sham. Bars represent group means ± SEM, $n=6$/group. $^{**}p<0.01$.

other hand, quantitative assessments of PC revealed marked increase in PC levels in tissue homogenate (~101%) over mitochondria (~45%) following SCI compared to sham, suggesting relatively lower protein oxidation in mitochondria (Fig. 4). Presence of BSA in the isolation buffer resulted in a very high PC band (~66 KD, indicated by arrows) in both sham and SCI groups in both tissue homogenate and mitochondrial fractions (Fig. 4A and B). Quantification of 4-HNE levels show that SCI did not alter lipid oxidation in either tissue homogenate (Fig. 5A) or mitochondria (Fig. 5B) at 24 h post-injury, with different two distinct antibodies (mouse monoclonal and rabbit polyclonal).

3.1.4. *Effects of SCI on LPO levels*

Consistent with results from 4-HNE assessments following SCI, there were no significant differences noted in either of the fractions in LPO levels compared to sham (Fig. 6).

3.1.5. *Effects of SCI on mitochondrial $O_2^{\bullet-}$ and H_2O_2 production:*

Measurement of superoxide anion was carried out using DCF fluorescence probe in freshly isolated mitochondria to show that contusion SCI significantly ($p<0.01$) increased production of superoxide anion compared to sham (Fig. 7A). Production of H_2O_2 was measured using highly-sensitive Amplex Red reagent, which reacts with H_2O_2 in the presence of peroxidase at a 1:1 ratio to produce the red-fluorescent oxidation product, resorufin. Compared to sham, significantly ($p<0.001$) higher H_2O_2 generation was observed in mitochondria after SCI (Fig. 7B).

Overall, our results show that in normal conditions, levels of antioxidant GSH and various oxidative stress parameters differ between rat spinal cord tissue homogenate and isolated mitochondrial fractions and that contusion spinal cord injury significantly and somewhat differentially decreased levels of GSH and increased all oxidative parameters except 4-HNE and LPO in both tissue homogenate and mitochondrial fractions at 24 h post-injury.

4. Discussion

This study undertook a comprehensive evaluation of ROS/RNS-mediated protein and lipid oxidation at cellular and subcellular levels following severe contusion SCI utilizing mitochondrial isolation procedures and quantifiable biochemical and molecular biological outcome measures of oxidative imbalance that can be widely used to evaluate potential antioxidant properties of experimental pharmacotherapeutics in cellular and subcellular fractions of spinal cord tissue following acute injury.

We first measured the levels of the most abundant endogenous antioxidant GSH in tissue homogenates and mitochondrial fractions since the role of GSH as a first line of defense against oxidative stress is well established [27]. GSH is synthesized primarily in the cytoplasm and then transported into the mitochondria through porin channels in the mitochondrial outer membrane [28]. Despite the quantitative differences in the cytosolic and mitochondrial GSH (mtGSH 10–15% of total GSH) pools, the mitochondrial pool is thought to play an important role in preserving cell viability following toxic insults compared with the cytosolic pool; probably due to high source of mitochondrial ROS generation which may interact with the redox-active thiol group of GSH [27,28]. A major function of GSH is to act as a scavenger of ROS/RNS either by the thiol or thiolate donating electrons or hydrogen atoms to free radicals to constitute oxidative repair processes, or by the thiolate reacting with electrophiles and recycling other antioxidants [27–29]. In the present study, depletion/oxidation of GSH in tissue homogenate and mitochondria indicates secondary pathophysiological events on cellular and subcellular GSH pools mediated by various ROS/RNS that oxidize GSH via trapping on thiol residues of GSH.

The pathophysiological secondary injury cascades following traumatic SCI are mediated by a series of cellular and biochemical events, such as glutamate excitotoxicity, Ca^{2+} influx, oxidative stress, inflammation, vascular events, and neuronal death [3,30]. Moreover, neurons are highly rich in mitochondria and are the highest energy consuming cell type; hence higher demand for mitochondrial ATP production. Mitochondria are a major source of ROS/RNS generation and are, therefore a potential therapeutic target [31,32]. Under high oxidative stress conditions observed after SCI, the endogenous antioxidant enzymes (e.g., SOD, catalase and peroxidase) and low molecular-weight antioxidants (e.g., glutathione, ascorbic acid, uric acid, lipoic acid and bilirubin) systems may become overwhelmed, consequently leading to redox imbalances. A number of studies have indicated free radical-mediated mitochondrial dysfunction as a significant contributor to secondary injury following SCI [9]. The mitochondrion is highly susceptible to oxidative damage following SCI, which can thereby lead to dysfunction of aerobic energy metabolism. Furthermore,

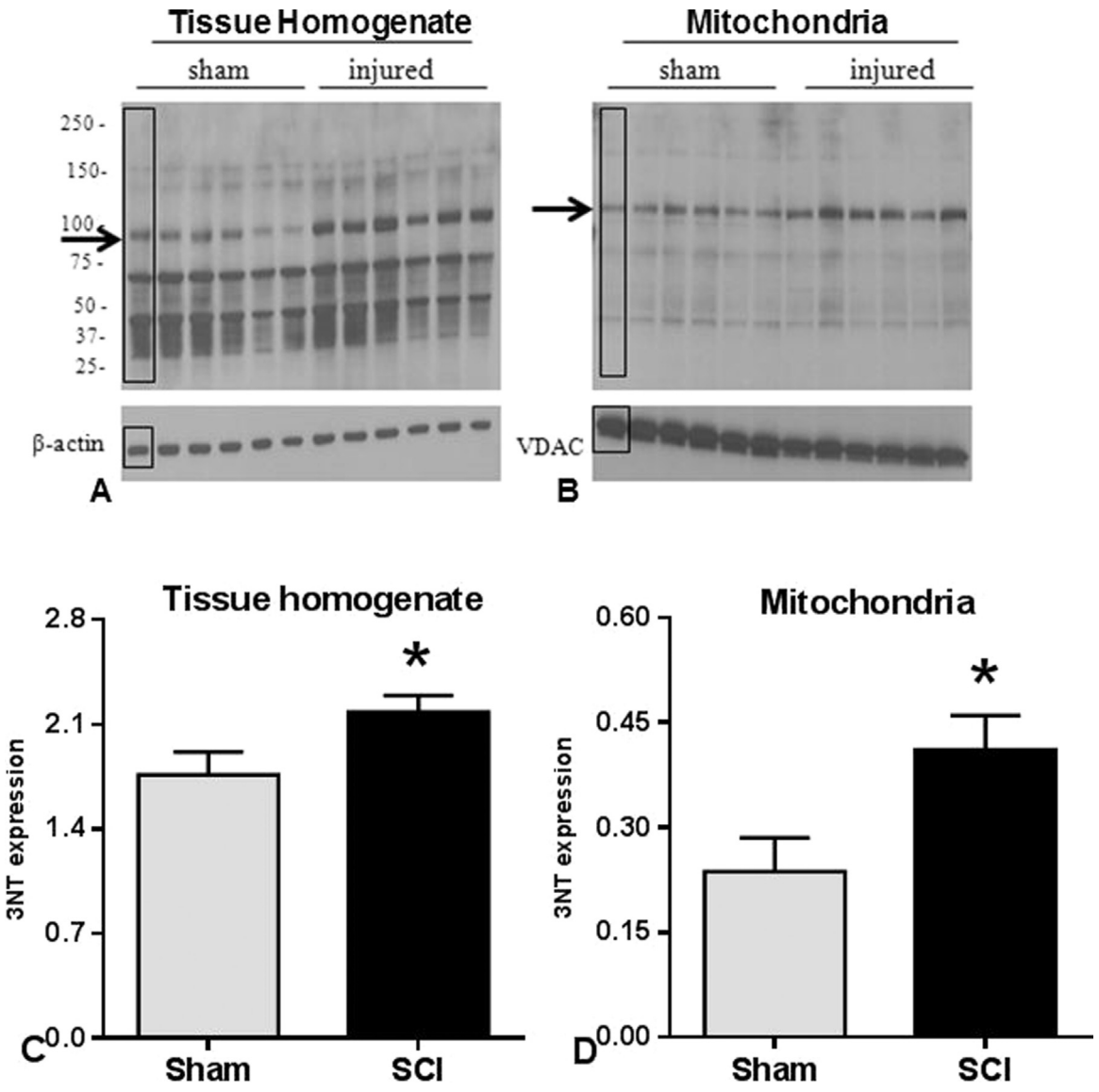

Fig. 3. Western blot images demonstrate 3-NT bands in tissue homogenate (A) and mitochondrial (B) fractions. Quantitative density values of 3-NT protein bands relative to internal controls from tissue homogenate (C) and mitochondrial fractions (D) showed that 24 h after SCI, 3-NT formation was significantly increased in both fractions compared to Shams. The boxes in A and B represent regions of interest used for comparative analyses. β-actin or VDAC were used as loading controls for tissue homogenate and mitochondria, respectively. Bars represent group means ± SEM, $n=6$/group. $^{*}p < 0.05$.

oxidative damage and mitochondrial dysfunction are interrelated processes which also catalyze other secondary injury events [1,3,30,31,33,34].

The majority of ROS and RNS, such as superoxide ($O_2^{\bullet -}$), nitric oxide ($NO^{\bullet}$), hydroxyl ($OH^{\bullet}$), peroxynitrite ($ONO\bar{O}$), hydrogen peroxide (H_2O_2), peroxyl ($ROO^{\bullet}$), and alkoxyl radicals ($RO^{\bullet}$) develop following pathological insults. Under normal physiological conditions, ROS/RNS have a dynamic equilibrium regulated by various enzymatic and non-enzymatic antioxidant systems. Under elevated levels of ROS and RNS production, however, these molecules may react with essential structural and functional components of cells such as fatty acids, proteins and DNA [19,35]. In this context, we documented high levels of $O_2^{\bullet -}$ and H_2O_2 generation in mitochondria following SCI. It is well documented that under normal physiological conditions, about 2–3% of electrons leak out from the mitochondrial electron transport chain (ETC). Other significant extramatrix and nonmitochondrial sources of ROS include cytochrome b_5 reductase, peroxisomes, catecholamines, hydroquinones, plasma membrane oxidases such as NADPH oxidase, lipoxygenases, monoamine oxidases, xanthine/xanthine oxidase, coupled or uncoupled nitric oxide synthase, and eicosanoids pathways, among others. Most of these compounds can initially lose an electron to form the superoxide anion radical ($O_2^{\bullet -}$) by autoxidation that can possibly contribute to cellular oxidative stress.

We have reported that compromised mitochondrial bioenergetics following contusion SCI is correlated with increased oxidative stress potentially due to increased ROS production [9,14]. Such production occurs within the mitochondrial matrix, intermembrane space, and outer membrane leading to the formation of H_2O_2 from reactions catalyzed by superoxide dismutase. H_2O_2 is membrane-permeable and a main precursor of hydroxyl radicals. H_2O_2 can react with transition metals through the Fenton reaction and the outcome is extremely reactive hydroxyl radical formation. Further, hydroxyl radicals along with peroxynitrite (also, intermediate radicals $CO_3^{\bullet -}$ and $^{\bullet}NO_2$) cause oxidative damage to downstream mitochondrial and cellular nucleic acids, protein, and lipid components [18,19,21,36,37].

We also found significant increases in $NO^{\bullet}$ production in tissue homogenate and mitochondrial fractions at 24 h following SCI.

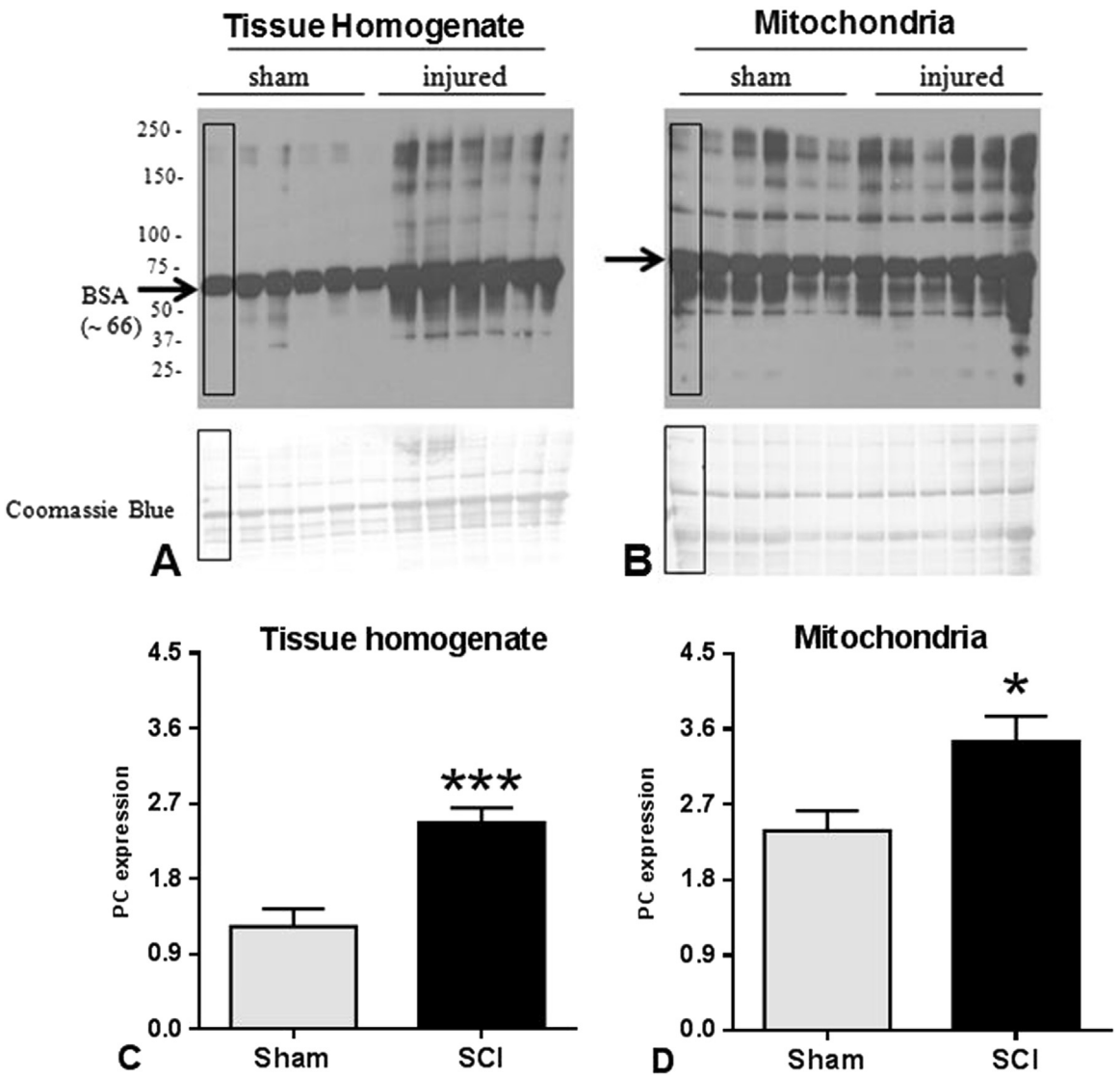

Fig. 4. Panels A and B represent western blot images for PC banding patterns in tissue homogenate and mitochondrial fractions, respectively. Quantitative results showed that after 24 h, SCI significantly increased PC formation in tissue homogenate (C) and mitochondrial fractions (D). The arrows in panels A and B indicate specific BSA bands of ~66 kDa that underwent carbonylation. The boxes in A and B represent regions of interest used for density calculations. As loading controls, transferred membranes were stained with Coomassie Blue and relative densities of PC levels for each sample were normalized to total protein loaded. Bars represent group means ± SEM, $n=6$/group. $^{*}p<0.05$; $^{***}p<0.001$.

$NO^{\bullet}$ is a highly diffusible and gaseous messenger molecule that participates in various physiological functions such as modulation of nociception, immune function and neurotransmission when at normal levels [38]. However, excessive $NO^{\bullet}$ production has cytotoxic effects and is implicated in neuronal injury after ischemia, trauma, and numerous neurodegenerative disorders [38]. Furthermore, there is evidence that high levels of intra-mitochondrial $NO^{\bullet}$ production can cause irreversible inhibition of oxygen consumption and ATP synthesis by competitive inhibition of cytochrome c oxidase, in addition to uncoupling, permeability transition, and/or cell death [39].

It is postulated that peroxynitrite derivative $^{\bullet}NO_2$ radical can nitrate the 3' position of tyrosine residues in proteins forming 3-NT which is a specific footprint of peroxynitrite-induced cellular damage [40]. Attention has also been focused on the oxidation of proteins thought to play a considerable role in neuropathology. The protein backbone and side-chains of most amino acids are susceptible to oxidation in the form of carbonyl formation associated with aging and neurodegenerative disorders, as well as in chronic inflammatory diseases, brain and spinal cord injury [36]. Although 3-NT and PC formation have been considered as biological markers for ROS/RNS, previous reports also suggest that unusual/modified amino acids are also potentially neurotoxic. For example, striatal injection of free 3-NT at concentrations similar to 6-hydroxydopamine, which causes a well described degenerative pathology and a Parkinsonian syndrome in rats, also induces selective loss of dopaminergic neurons [41].

Disruption of mitochondrial ETC function leads to excessive production of $O_2^{\bullet-}$ and H_2O_2, which can produce the highly toxic $OH^{\bullet}$ radicals via the metal-catalyzed Fenton/ Haber–Weiss reaction. Elevated $O_2^{\bullet-}$ also rapidly reacts with $NO^{\bullet}$ to form $ONOO^{-}$. The protonated form of peroxynitrite (ONOOH) is a powerful oxidizing agent which causes damage to many biological molecules. Furthermore, CO_2 is readily available in mitochondria due to the decarboxylation reactions catalyzed by pyruvate dehydrogenase (PDH) and in the Krebs cycle, and can react with peroxynitrite to produce carbonate ($CO_3^{\bullet-}$) and nitrogen dioxide ($^{\bullet}NO_2$) intermediates, less potent radicals. A minor amount of peroxynitrite can also undergo the proton-catalyzed homolysis to yield $^{\bullet}OH$ and $^{\bullet}NO_2$. All of these processes occurring in intra-mitochondrial

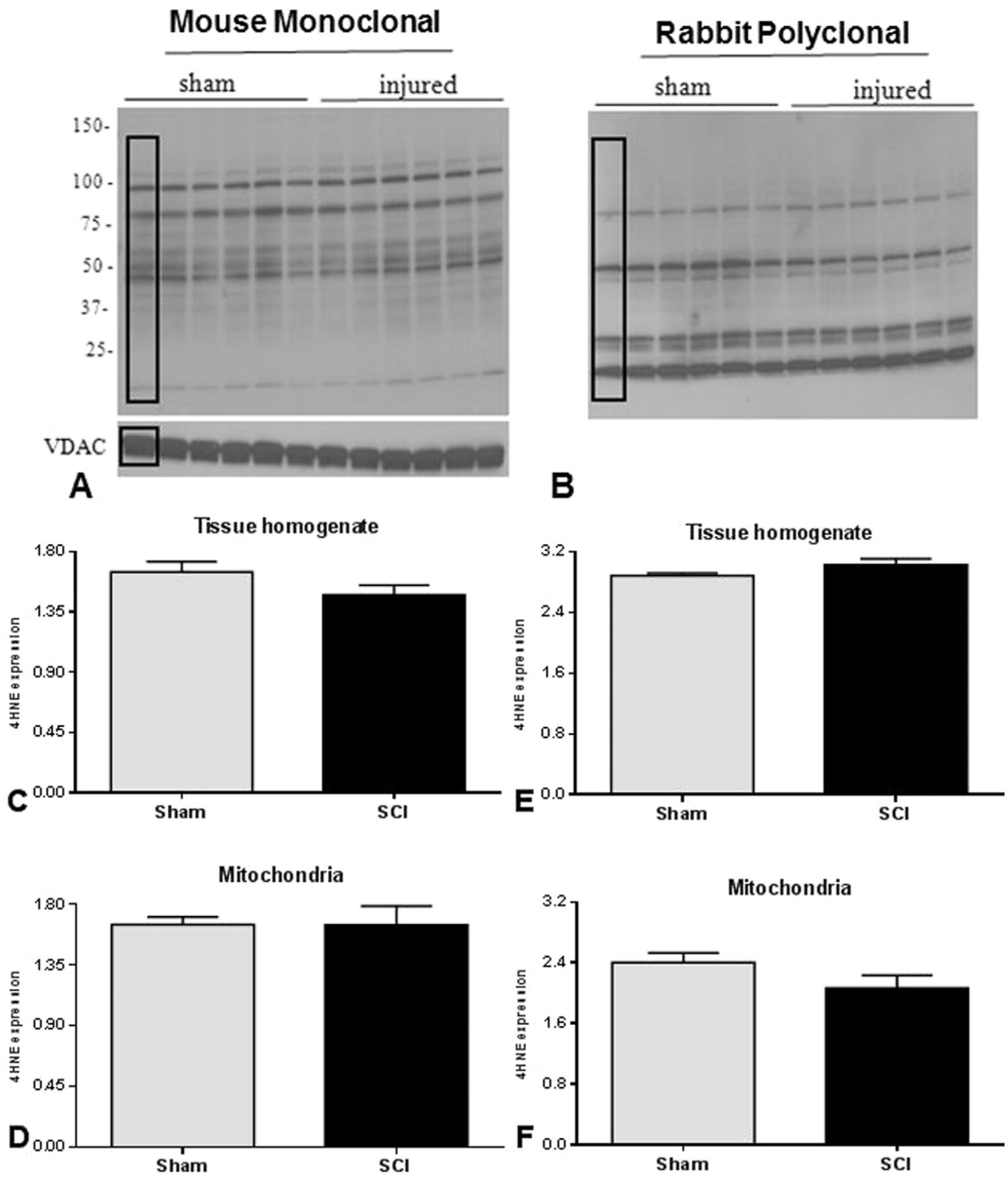

Fig. 5. Representative western blots demonstrate 4-HNE adducts formation using mouse monoclonal (A) and rabbit polyclonal (B) antibodies for mitochondrial fractions, using VDAC as a loading control. The bar graphs show that there were no changes in 4-HNE levels 24 h after SCI compared to Sham using either antibody in tissue homogenate (C and E) or mitochondrial (D and H) fractions. It should be noted that the PVDF membrane for mitochondria was stripped prior to re-probe with VDAC and then again for rabbit polyclonal antibody; hence a common VDAC band was used for normalization of both 4-HNE antibodies. The boxes in A and B represent regions of interest used for density calculations. Bars represent group means ± SEM, $n=6$/group.

compartments result in oxidation, nitration, and nitrosylation of critical components of the matrix, inner and outer membranes, and inter-membrane space; subsequently this damage is attributed to various toxic formations of lipids, proteins and nucleic acids [3,42–44].

Oxidative stress in neuronal injury is a hallmark of pathology since the spinal cord contains a relatively large volume of polyunsaturated fatty acids (PUFAs) (e.g., linoleic acid and arachidonic acid) that are highly susceptible to lipid-derived oxidative stress, specifically lipid peroxidation processes [31]. Accordingly, a highly toxic aldehydic product of lipid peroxidation is 4-HNE, which has been well characterized in experimental brain and spinal cord injury models, and can covalently bind to basic amino acids (e.g., lysine, histidine, arginine, cysteine) to modify the protein structure and functional properties that can alter mitochondrial bioenergetics [1,40,45]. The present study investigated concomitant cellular and subcellular (mitochondrial) levels of oxidative markers following a more severe contusion SCI at L1/L2 spinal levels. Interestingly, our findings demonstrate that a specific ~95 kDa mitochondrial protein is susceptible to 3-NT formation. Furthermore, we observed that PC formation was significantly increased in the 70 to 250 kDa mitochondrial protein range. However, we are

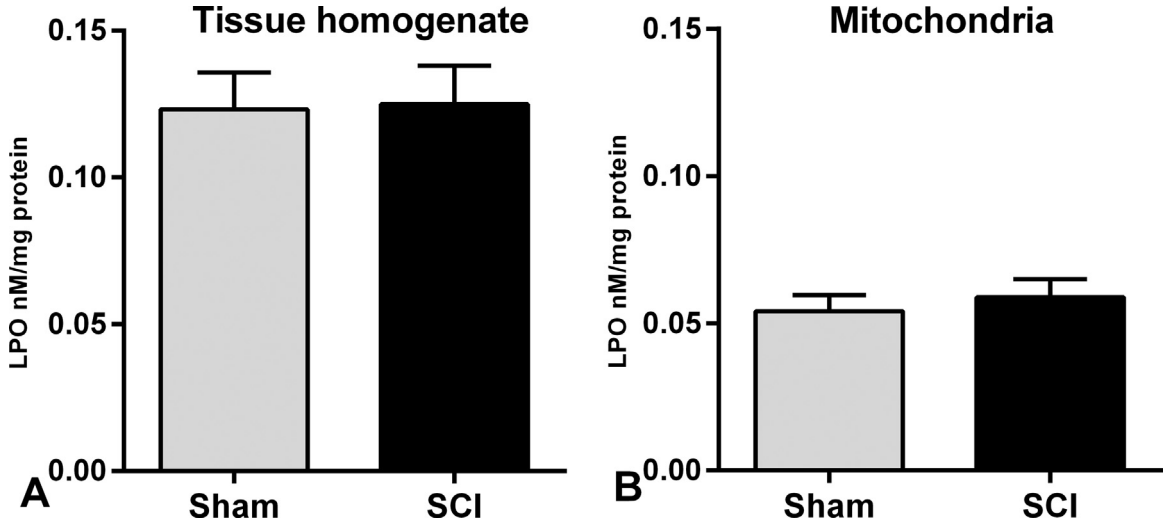

Fig. 6. LPO levels that were measured by TBA–TCA reagent were not different in either tissue homogenate (A) or mitochondrial (B) fractions 24 h following contusion SCI compared to Shams. Bars represent group means ± SEM, $n=6$/group.

uncertain about the specific mitochondrial protein(s) susceptible to 3-NT and PC formation following SCI. Conversely, we could not find any remarkable changes in 4-HNE levels employing two different sources of antibodies or in LPO formation in injured cellular or subcellular fractions compared to shams.

Using Western blot analysis, previous studies have demonstrated that 4-HNE rapidly increases in spinal cord tissue homogenate fractions following T10 contusion SCI in female Long-Evans rats at early time points after injury (1, 4 and 24 h) [12]. Another time course study revealed that all three oxidative stress markers (i.e., 3-NT, PC and 4-HNE) were increased in spinal cord tissue homogenate [13] and in isolated mitochondria [9] following T10 contusion SCI in female Sprague-Dawley rats using slot blot immunolabeling. Compared to former studies documenting 4-HNE formation in thoracic SCI models [12,13], our differential results may stem from injury site of our model (L1/L2) that consist of relatively higher gray matter/white matter ratio compared to T10 spinal level, their previous usage of different immuno-slot blot techniques, antibody sources, isolation buffers, as well as forces applied. Using western blot analysis we have previously shown significantly higher levels of 4-HNE in spinal cord mitochondria compared to cortex from naïve adult Sprague-Dawley rats [46]. Therefore, it is possible that higher lipid peroxidation under normal conditions led to a ceiling effect, which may explain why we are not observing increases 24 h after SCI.

Overall, the present study shows that after contusion SCI there is significantly increased GSH oxidation paralleled by production of $O_2^{\bullet-}$, H_2O_2 and $NO^{\bullet}$, and likely its derivatives (i.e. peroxynitrite, nitrogen dioxide, hydroxyl radical or carbonate), which all play important roles in induction of oxidative stress at cellular and/or subcellular levels. In addition, we demonstrate increased nitration and oxidation of proteins (3-NT and PC, respectively) at 24 h after SCI in both the fractions. Hence, results from the current study support the critical role of free radical–mediated secondary injury cascades after SCI, including toxic oxidative damage at cellular and subcellular levels. From these insights, pharmacotherapeutic strategies that specifically target oxidants generated at sub-cellular (mitochondrial) and cellular levels are the next logical target to be explored for promoting functional neuroprotection after traumatic SCI.

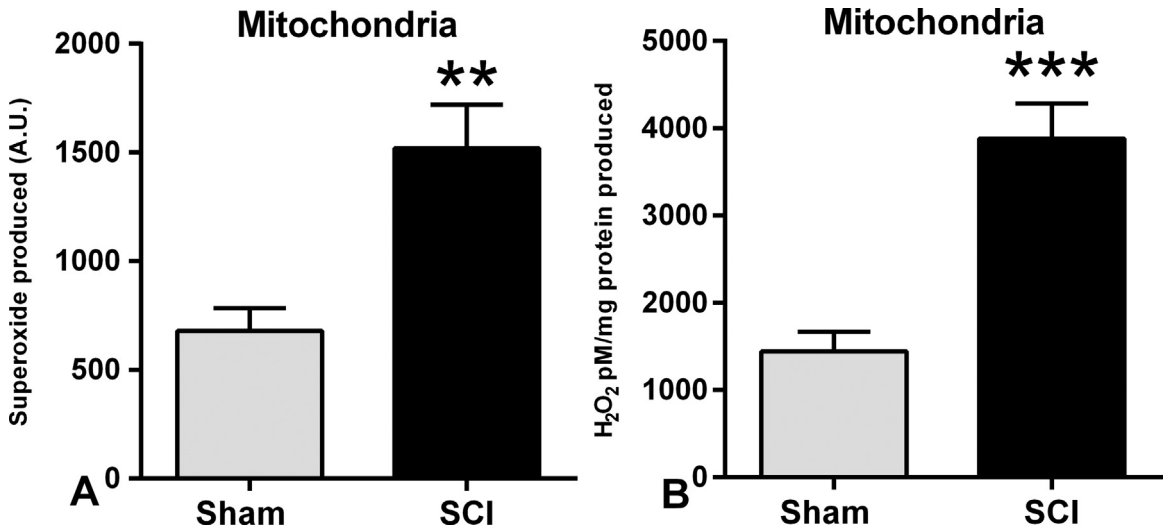

Fig. 7. Production of superoxide radical ($O_2^{\bullet-}$) in mitochondria was measured using DCF/HRP fluorescence dye. $O_2^{\bullet-}$ production was significantly increased in mitochondrial fractions (A) at 24 h after SCI compared with Shams. Production of hydrogen peroxide (H_2O_2) in mitochondria was measured using Amplex Red/HRP fluorescence reagent and was also found to be significantly increased 24 h after SCI (B) compared to Shams. Bars represent group means ± SEM, $n=6$/group. $^{**}p<0.01$; $^{***}p<0.001$.

Conflict of interest statement

No conflict of interests exists for any authors.

Acknowledgments

We are grateful to Dr. Edward D. Hall for generously providing rabbit polyclonal anti-HNE antibody. Special thanks to Mr. Taylor Smith and Mr. David Cox for pre- and post-operative animal care. This study was supported by NIH/NINDS R01NS069633 (A.G.R. and P.G.S.), The Craig H. Neilsen Foundation 260771 (S.P.), The Craig H. Neilsen Foundation 190115 (A.G.R.) and NIH/NINDS P30 NS051220 (E.D.H).

References

[1] M. Bains, E.D. Hall, Antioxidant therapies in traumatic brain and spinal cord injury, Biochim. Biophys. Acta 1822 (2012) 675–684.
[2] G. Fatima, V.P. Sharma, S.K. Das, A.A. Mahdi, Oxidative stress and antioxidative parameters in patients with spinal cord injury: implications in the pathogenesis of disease, Spinal Cord 53 (2015) 3–6.
[3] E.D. Hall, J.E. Springer, Neuroprotection and acute spinal cord injury: a reappraisal, NeuroRx: J. Am. Soc. Exp. Neurother. 1 (2004) 80–100.
[4] M.L. McEwen, P.G. Sullivan, A.G. Rabchevsky, J.E. Springer, Targeting mitochondrial function for the treatment of acute spinal cord injury, Neurother.: J. Am. Soc. Exp. Neurother. 8 (2011) 168–179.
[5] A.G. Rabchevsky, S.P. Patel, J.E. Springer, Pharmacological interventions for spinal cord injury: where do we stand? How might we step forward? Pharmacol. Ther. 132 (2011) 15–29.
[6] J.E. Springer, R.R. Rao, H.R. Lim, S.I. Cho, G.J. Moon, H.Y. Lee, E.J. Park, J.S. Noh, B. J. Gwag, The functional and neuroprotective actions of Neu2000, a dual-acting pharmacological agent, in the treatment of acute spinal cord injury, J. Neurotrauma 27 (2010) 139–149.
[7] D.P. Kuffler, Maximizing neuroprotection: where do we stand? Ther. Clin. Risk Manag. 8 (2012) 185–194.
[8] M.L. McEwen, P.G. Sullivan, J.E. Springer, Pretreatment with the cyclosporin derivative, NIM811, improves the function of synaptic mitochondria following spinal cord contusion in rats, J. Neurotrauma 24 (2007) 613–624.
[9] P.G. Sullivan, S. Krishnamurthy, S.P. Patel, J.D. Pandya, A.G. Rabchevsky, Temporal characterization of mitochondrial bioenergetics after spinal cord injury, J. Neurotrauma 24 (2007) 991–999.
[10] P.G. Sullivan, A.G. Rabchevsky, P.C. Waldmeier, J.E. Springer, Mitochondrial permeability transition in CNS trauma: cause or effect of neuronal cell death? J. Neurosci. Res. 79 (2005) 231–239.
[11] M. Aksenova, D.A. Butterfield, S.X. Zhang, M. Underwood, J.W. Geddes, Increased protein oxidation and decreased creatine kinase BB expression and activity after spinal cord contusion injury, J. Neurotrauma 19 (2002) 491–502.
[12] J.E. Springer, R.D. Azbill, R.J. Mark, J.G. Begley, G. Waeg, M.P. Mattson, 4-Hydroxynonenal, a lipid peroxidation product, rapidly accumulates following traumatic spinal cord injury and inhibits glutamate uptake, J. Neurochem. 68 (1997) 2469–2476.
[13] Y. Xiong, A.G. Rabchevsky, E.D. Hall, Role of peroxynitrite in secondary oxidative damage after spinal cord injury, J. Neurochem. 100 (2007) 639–649.
[14] S.P. Patel, P.G. Sullivan, J.D. Pandya, A.G. Rabchevsky, Differential effects of the mitochondrial uncoupling agent, 2,4-dinitrophenol, or the nitroxide antioxidant, Tempol, on synaptic or nonsynaptic mitochondria after spinal cord injury, J. Neurosci. Res. 87 (2009) 130–140.
[15] S.P. Patel, P.G. Sullivan, T.S. Lyttle, D.S. Magnuson, A.G. Rabchevsky, Acetyl-L-carnitine treatment following spinal cord injury improves mitochondrial function correlated with remarkable tissue sparing and functional recovery, Neuroscience 210 (2012) 296–307.
[16] S.P. Patel, P.G. Sullivan, J.D. Pandya, G.A. Goldstein, J.L. VanRooyen, H. M. Yonutas, K.C. Eldahan, J. Morehouse, D.S. Magnuson, A.G. Rabchevsky, N-acetylcysteine amide preserves mitochondrial bioenergetics and improves functional recovery following spinal trauma, Exp. Neurol. 257 (2014) 95–105.
[17] S.W. Scheff, A.G. Rabchevsky, I. Fugaccia, J.A. Main, J.E. Lumpp Jr., Experimental modeling of spinal cord injury: characterization of a force-defined injury device, J. Neurotrauma 20 (2003) 179–193.
[18] M.P. Murphy, How mitochondria produce reactive oxygen species, Biochem. J. 417 (2009) 1–13.
[19] D.F. Stowe, A.K. Camara, Mitochondrial reactive oxygen species production in excitable cells: modulators of mitochondrial and cell function, Antioxid. Redox Signal. 11 (2009) 1373–1414.
[20] V.J. Thannickal, B.L. Fanburg, Reactive oxygen species in cell signaling, Am. J. Physiol. Lung Cell. Mol. Physiol. 279 (2000) L1005–L1028.
[21] J.F. Turrens, Mitochondrial formation of reactive oxygen species, J. Physiol. 552 (2003) 335–344.
[22] J.C. Fernandez-Checa, N. Kaplowitz, The use of monochlorobimane to determine hepatic GSH levels and synthesis, Anal. Biochem. 190 (1990) 212–219.
[23] J.A. Buege, S.D. Aust, Microsomal lipid peroxidation, Methods Enzym. 52 (1978) 302–310.
[24] T. Ullrich, S. Oberle, A. Abate, H. Schroder, Photoactivation of the nitric oxide donor SIN-1, FEBS Lett. 406 (1997) 66–68.
[25] N.P. Visavadiya, M.L. McEwen, J.D. Pandya, P.G. Sullivan, B.J. Gwag, J.E. Springer, Antioxidant properties of Neu2000 on mitochondrial free radicals and oxidative damage, Toxicol. Vitro: Int. J. Publ. Assoc. BIBRA 27 (2013) 788–797.
[26] P.R. Castello, D.A. Drechsel, B.J. Day, M. Patel, Inhibition of mitochondrial hydrogen peroxide production by lipophilic metalloporphyrins, J. Pharmacol. Exp. Ther. 324 (2008) 970–976.
[27] M.P. Murphy, Mitochondrial thiols in antioxidant protection and redox signaling: distinct roles for glutathionylation and other thiol modifications, Antioxid. Redox Signal. 16 (2012) 476–495.
[28] M. Mari, A. Morales, A. Colell, C. Garcia-Ruiz, J.C. Fernandez-Checa, Mitochondrial glutathione, a key survival antioxidant, Antioxid. Redox Signal. 11 (2009) 2685–2700.
[29] V.I. Lushchak, Glutathione homeostasis and functions: potential targets for medical interventions, J. Amino Acids 2012 (2012) 736837.
[30] D.K. Anderson, E.D. Hall, Pathophysiology of spinal cord trauma, Ann. Emerg. Med. 22 (1993) 987–992.
[31] E.D. Hall, Lipid peroxidation discussion 257-248, Adv. Neurol. 71 (1996) 247–257.
[32] T.L. Schwarz, Mitochondrial trafficking in neurons, Cold Spring Harb. Perspect. Biol. 5 (2013).
[33] E.D. Hall, J.M. Braughler, Free radicals in CNS injury, Res. Publ. Assoc. Res. Nerv. Ment. Disord. 71 (1993) 81–105.
[34] P.G. Sullivan, M.R. Brown, Mitochondrial aging and dysfunction in Alzheimer's disease, Prog. Neuro Psychopharmacol. Biol. Psychiatry 29 (2005) 407–410.
[35] R. Kohen, A. Nyska, Oxidation of biological systems: oxidative stress phenomena, antioxidants, redox reactions, and methods for their quantification, Toxicol. Pathol. 30 (2002) 620–650.
[36] S. Adams, P. Green, R. Claxton, S. Simcox, M.V. Williams, K. Walsh, C. Leeuwenburgh, Reactive carbonyl formation by oxidative and non-oxidative pathways, Front. Biosci.: J. Virtual Libr. 6 (2001) A17–A24.
[37] M.W. Fariss, C.B. Chan, M. Patel, B. Van Houten, S. Orrenius, Role of mitochondria in toxic oxidative stress, Mol. Interv. 5 (2005) 94–111.
[38] A. Conti, M. Miscusi, S. Cardali, A. Germano, H. Suzuki, S. Cuzzocrea, F. Tomasello, Nitric oxide in the injured spinal cord: synthases cross-talk, oxidative stress and inflammation, Brain Res. Rev. 54 (2007) 205–218.
[39] G.C. Brown, Regulation of mitochondrial respiration by nitric oxide inhibition of cytochrome c oxidase, Biochim. Biophys. Acta 1504 (2001) 46–57.
[40] E.D. Hall, J.A. Wang, J.M. Bosken, I.N. Singh, Lipid peroxidation in brain or spinal cord mitochondria after injury, J. Bioenerg. Biomembr. (2015).
[41] M.J. Mihm, B.L. Schanbacher, B.L. Wallace, L.J. Wallace, N.J. Uretsky, J.A. Bauer, Free 3-nitrotyrosine causes striatal neurodegeneration in vivo, J. Neurosci.: Off. J. Soc. Neurosci. 21 (2001) RC149.
[42] R. Radi, A. Cassina, R. Hodara, C. Quijano, L. Castro, Peroxynitrite reactions and formation in mitochondria, Free. Radic. Biol. Med. 33 (2002) 1451–1464.
[43] C. Szabo, H. Ischiropoulos, R. Radi, Peroxynitrite: biochemistry, pathophysiology and development of therapeutics, Nat. Rev. Drug. Discov. 6 (2007) 662–680.
[44] D.B. Zorov, M. Juhaszova, S.J. Sollott, Mitochondrial reactive oxygen species (ROS) and ROS-induced ROS release, Physiol. Rev. 94 (2014) 909–950.
[45] R.A. Vaishnav, I.N. Singh, D.M. Miller, E.D. Hall, Lipid peroxidation-derived reactive aldehydes directly and differentially impair spinal cord and brain mitochondrial function, J. Neurotrauma 27 (2010) 1311–1320.
[46] P.G. Sullivan, A.G. Rabchevsky, J.N. Keller, M. Lovell, A. Sodhi, R.P. Hart, S. W. Scheff, Intrinsic differences in brain and spinal cord mitochondria: implication for therapeutic interventions, J. Comp. Neurol. 474 (2004) 524–534.